AD-A084 674 DAVID W TAYLOR NAVAL SHIP RESEARCH AND DEVELOPMENT CE--ETC F/G 13/10
A NONLINEAR FREQUENCY DOMAIN SIMULATION FOR SWATH CRAFT,(U)
MAR 80 W H LIVINGSTON
UNCLASSIFIED DTNSRDC/SPD-0893-01 NL

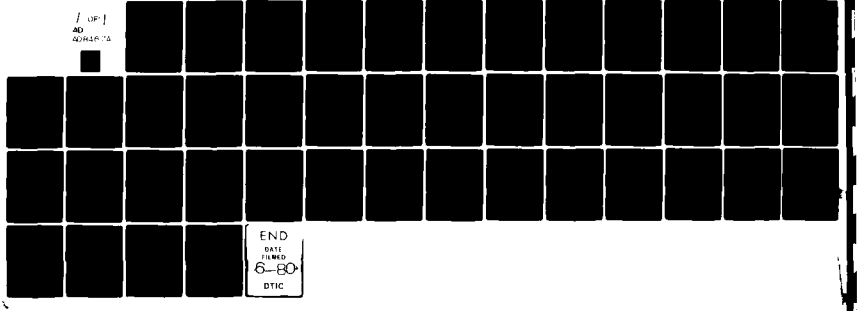

END
DATE FILMED
6-80
DTIC

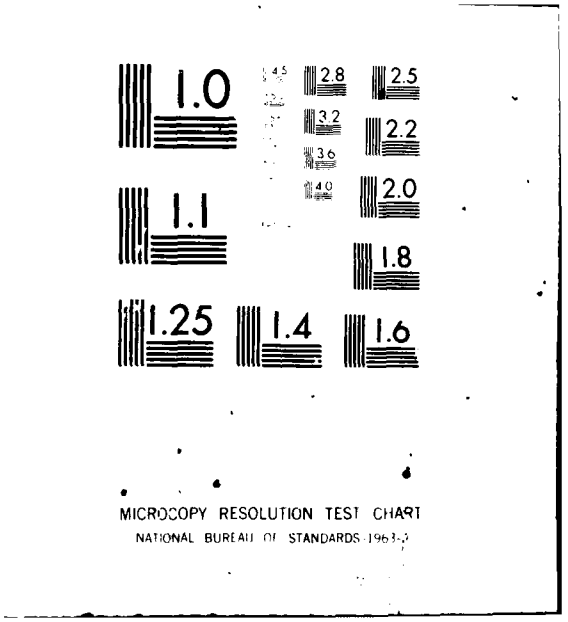
1.0
2.8
2.5
3.2
2.2
3.6
2.0
4.0
1.1
1.8
1.25
1.4
1.6
MICROCOPY RESOLUTION TEST CHART
NATIONAL BUREAU OF STANDARDS-1963-A

DAVID W. TAYLOR NAVAL SHIP RESEARCH AND DEVELOPMENT CENTER

Bethesda, Md. 20084

A NONLINEAR FREQUENCY DOMAIN SIMULATION FOR SWATH CRAFT

by

WALTER LIVINGSTON

SHIP PERFORMANCE DEPARTMENT

MARCH 1980

DTNSRDC/SPD-0893-01

A NONLINEAR FREQUENCY DOMAIN SIMULATION FOR SWATH CRAFT

MAJOR DTNSRDC ORGANIZATIONAL COMPONENTS

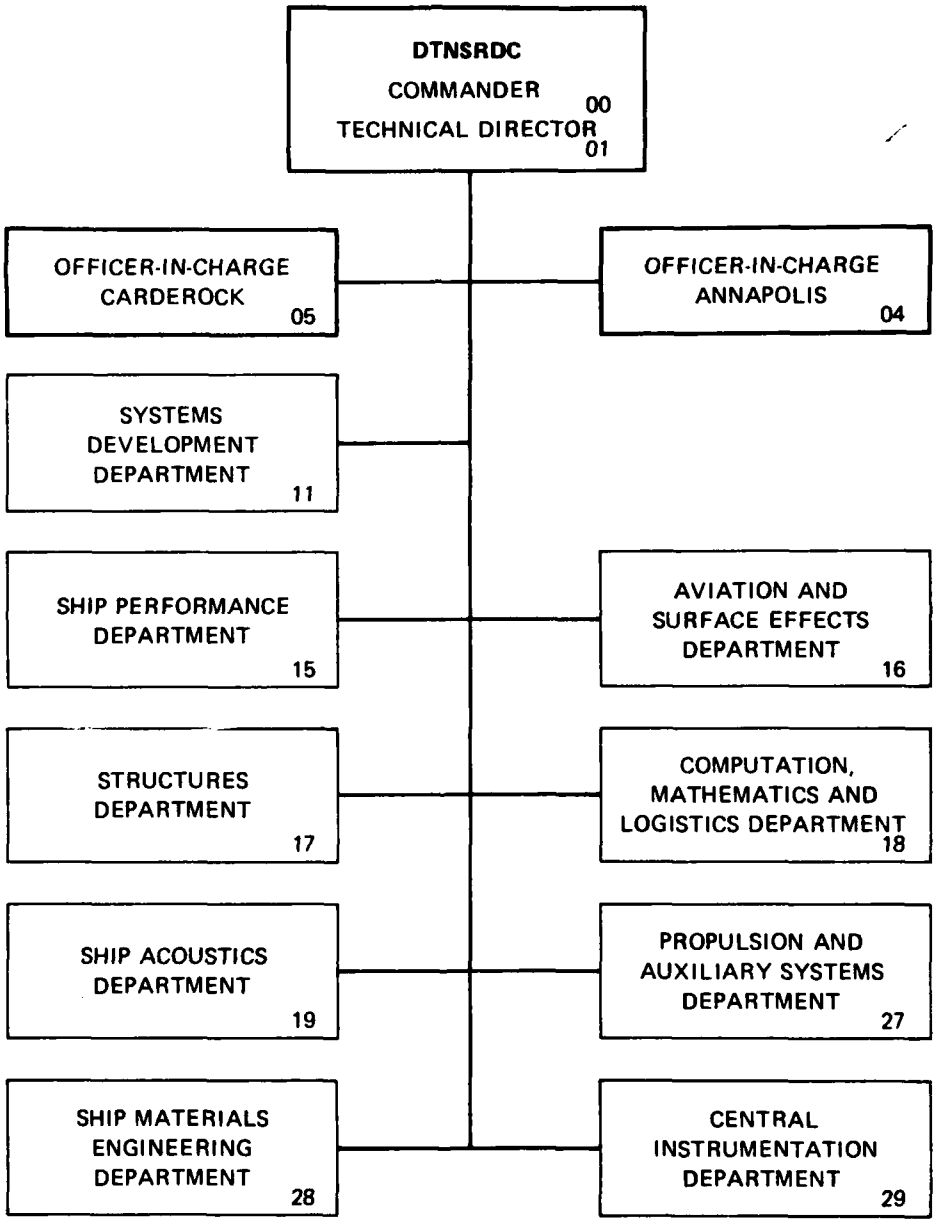

UNCLASSIFIED

SECURITY CLASSIFICATION OF THIS PAGE (When Data Entered)

REPORT DOCUMENTATION PAGE		READ INSTRUCTIONS BEFORE COMPLETING FORM
1. REPORT NUMBER DTNSRDC/SPD-0893-01	2. GOVT ACCESSION NO. AD-A084 674	3. RECIPIENT'S CATALOG NUMBER
4. TITLE (and Subtitle) A Nonlinear Frequency Domain Simulation for SWATH Craft		5. TYPE OF REPORT & PERIOD COVERED 6. PERFORMING ORG. REPORT NUMBER
7. AUTHOR(s) Walter H. Livingston		8. CONTRACT OR GRANT NUMBER(s)
9. PERFORMING ORGANIZATION NAME AND ADDRESS David W. Taylor Naval Ship Research and Development Center Bethesda, MD 20084		10. PROGRAM ELEMENT, PROJECT, TASK AREA & WORK UNIT NUMBERS 61153N SR0230101 and ZF43-421 1-1572-145
11. CONTROLLING OFFICE NAME AND ADDRESS General Hydromechanics Research Program Naval Material Command (08T)		12. REPORT DATE MARCH 1980 13. NUMBER OF PAGES 42
14. MONITORING AGENCY NAME & ADDRESS(if different from Controlling Office)		15. SECURITY CLASS. (of this report) UNCLASSIFIED 15a. DECLASSIFICATION/DOWNGRADING SCHEDULE

16. DISTRIBUTION STATEMENT (of this Report)

APPROVED FOR PUBLIC RELEASE: DISTRIBUTION UNLIMITED

17. DISTRIBUTION STATEMENT (of the abstract entered in Block 20, if different from Report)

18. SUPPLEMENTARY NOTES

19. KEY WORDS (Continue on reverse side if necessary and identify by block number)

Nonlinear, Frequency Domain, Simulation, SWATH Craft, Controller.

20. ABSTRACT (Continue on reverse side if necessary and identify by block number)

The development of a nonlinear frequency domain simulation which accomodates frequency independent nonlinearities is described. Although developed around the dynamics of a particular naval craft, the simulation can be applied to the most general situation and need not be restricted solely to the prediction of ship motions. The workability and usefulness of the simulation is demonstrated by carrying out three scenarios with the SWATH 6A craft. Two scenarios are open loop; the third includes automatic control. These scenarios are also simulated in the time domain using a

DD FORM 1 JAN 73 1473 EDITION OF 1 NOV 65 IS OBSOLETE
S/N 0102-014-6601

UNCLASSIFIED

SECURITY CLASSIFICATION OF THIS PAGE (When Data Entered)

generalized nonlinear time domain simulation which is based on the same modeling of the craft dynamics that is used for the nonlinear frequency domain simulation. The results obtained with these simulations agree for each of the scenarios simulated.

When the results obtained with the nonlinear frequency domain simulation are contrasted with those obtained with a linear frequency domain simulation which employs equivalent linearization, the lack of agreement is noticeable. This highlights the limited usefulness of equivalent linearization.

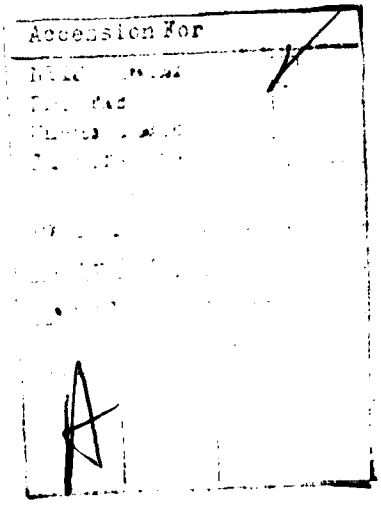

TABLE OF CONTENTS

	Page
LIST OF FIGURES	iii
NOTATION	v
ABSTRACT	1
ADMINISTRATIVE INFORMATION	1
INTRODUCTION	1
COORDINATE SYSTEM	2
SWATH CRAFT SYSTEM DYNAMICS MODELING	3
FREQUENCY INDEPENDENT NONLINEARITIES	5
NONLINEARITIES MODELED IN THE SWATH 6A DYNAMICS	5
NONLINEAR FREQUENCY DOMAIN SIMULATION	10
SCENARIOS SIMULATED	13
PRESENTATION OF RESULTS	14
CONCLUSIONS	24
ACKNOWLEDGMENTS	24
REFERENCES	27
APPENDIX - SEAWAY DESCRIPTION	29

LIST OF FIGURES

1 - Velocity Vector involved in Computing Lift and Drag	8
2 - Flowchart for the Fin Angle Controller	9
3 - Flowchart for the Nonlinear Frequency Domain Simulation	12
4 - Heave Amplitude for Scenarios 1 and 2	16
5 - Heave Phase for Scenarios 1 and 2	17
6 - Pitch Angle Amplitude for Scenarios 1 and 2	18

LIST OF FIGURES (CONT)

	Page
7 - Pitch Angle Phase for Scenarios 1 and 2	19
8 - Heave Amplitude for Scenario 3.	20
9 - Heave Phase for Scenario 3.	21
10 - Pitch Angle Amplitude for Scenario 3.	22
11 - Pitch Phase Angle for Scenario 3.	23
12 - Time History of One Cycle of Fin Order and Fin Displacement Under Automatic Control.	25
13 - Time History of One Cycle of Heave Displacement With and Without Controller	26
14 - Pierson-Moskowitz Energy Spectrum for a Sea State 6	32

NOTATION*

A_{FR}	Area of R^{th} Fin
a_o	Constant used in formula for viscous lift on hulls
A_{PBM}	Projected Area of M^{th} Hull Section
A_{33}	Frequency Dependent Coefficient
A_{35}	Frequency Dependent Coefficient
A_{53}	Frequency Dependent Coefficient
A_{55}	Frequency Dependent Coefficient
B_{33}	Frequency Dependent Coefficient
B_{35}	Frequency Dependent Coefficient
B_{53}	Frequency Dependent Coefficient
B_{55}	Frequency Dependent Coefficient
C_{DBM}	Cross Flow Drag Coefficient for M^{th} Hull Section
C_{DFR}	Cross Flow Drag Coefficient for R^{th} Fin
C_{LFR_α}	Lift Coefficient for R^{th} Fin
C_{33}	Frequency Independent Coefficient
C_{35}	Frequency Independent Coefficient
C_{53}	Frequency Independent Coefficient
C_{55}	Frequency Independent Coefficient
D_{BM}	Cross Flow Drag of M^{th} Hull Section
D_{FR}	Cross Flow Drag of R^{th} Fin
$\bar{F}$	Complex Amplitude of Wave Exciting Force in Heave
$\bar{E}(\omega)$	Total Force Vector in Frequency Domain
$\bar{E}'(\omega)$	Force Input to System Transfer Matrix

*Note - Much of this notation is taken from Reference 1 and is used here without change

$\underline{\bar{F}}_{EXT}(\omega)$	External Force Vector
$\bar{F}_{NL}(t)$	Vector of Nonlinear Motion Dependent Forces in Time Domain
$\underline{\bar{F}}_{NL}(\omega)$	Vector of Nonlinear Motion Dependent Forces in Frequency Domain
$\underline{\bar{F}}_{o}(\omega)$	Initial Value for $F(\omega)$
$\underline{\bar{F}}_{1}(\omega)$	Current Value of Force Vector Minus Initial Value
$\underline{\bar{F}}_{OLD}(\omega)$	$\underline{\bar{F}}(\omega)$ from Previous Iteration
FFT	Fast Fourier Transform
FFT^{-1}	Inverse Fast Fourier Transform
$[\bar{G}(\omega)]$	A Matrix Involved in Computing $[\bar{\alpha}(\omega)]$
g	Acceleration Due to Gravity
$[\bar{H}(\omega)]$	System Transfer Matrix
$\bar{H}_{33}(\omega)$	Frequency Response Function
$\bar{H}_{35}(\omega)$	Frequency Response Function
$\bar{H}_{53}(\omega)$	Frequency Response Function
$\bar{H}_{55}(\omega)$	Frequency Response Function
$H_{1/3}$	Significant Wave Height in meters
I_5	Mass Moment of Inertia of Craft About the Y_0-Axis
j	Square Root of -1
$L_{BM}(t)$	Viscous Lift at the M^{th} Hull Section
$L_{FR}(t)$	Lift of the R^{th} Fin
M	Inertial Mass of the Craft
$P(\omega)$	Energy Ordinate of the Seaway Energy Spectrum at ω
$\bar{T}(\omega)$	Complex Amplitude of Wave Exciting Moment in Heave
t	Time

NOTATION (CONT)

U_o	Constant Mean Forward Velocity of Ship
V_{BM}	Local Total Velocity at the M^{th} Hull Section
V_{FR}	Local Total Velocity at the R^{th} Fin
V_W	Wind Speed in Knots
$\underline{\overline{X}}(\omega)$	Motion Vector in the Frequency Domain
$\overline{X}(t)$	Motion Vector in the Time Domain
$\underline{\overline{X}}_o(\omega)$	Motion Vector at $Zero^{th}$ Iteration
$\underline{\overline{X}}_1(\omega)$	The Current Value of the Motion Vector Minus the Initial Value
X_{OBM}	Location of the M^{th} Hull Section
X_{OFR}	Location of the R^{th} Fin
$X_oY_oZ_o$	Inertial Coordinate System Moving at the Mean (Constant) Forward Velocity of the Craft. Motions of the Craft are Assumed to be Perturbations About this Axis System
$\overline{Z}_{oa}$	Amplitude of Heave Response of Craft to a Sinusoidal Input
$\alpha_{BM}(t)$	Local Angle of Attack at M^{th} Hull Section
$\alpha_{FR}(t)$	Local Angle of Attack at R^{th} Fin
β	Seaway Heading, $\beta = 0^o$ for Following Seas; $\beta = 180^o$ for Head Seas
$\overline{\varepsilon}(\omega)$	Vector of Convergence Criteria
θ	Pitch Angle
$\overline{\theta}_a$	Complex Amplitude of Pitch Response of Craft to a Sinusoidal Input
$\delta_{ORD_i}(KT)$	Ordered Fin Angle on i^{th} Iteration
δ_{MAX}	Maximum Fin Angle
$\delta(KT)$	Time Series for Fin Angle Deflection

NOTATION (CONT)

$\dot{\delta}_{MAX}$	Maximum Fin Angle Rate
τ	Time Constant
T	Sampling Time Interval
$\Omega_i (1 \leq i \leq 12)$	Phase Angle Selected from a Uniform Distribution (Random) over 0 to 2 π and Added to Wave Angular Frequency
ω	Encounter Frequency
ω_i	The i^{th} Wave Angular Frequency
$\gamma_i (1 \leq i \leq 15)$	Random Phase Angles
ρ	Mass Density of Seawater
$\dot{\zeta}_{X_{OBM_i}}(t)$	Wave Orbital Velocity in the X_o Direction at the M^{th} Hull Section and for the i^{th} Wave
$\dot{\zeta}_{X_{OFR_i}}(t)$	Wave Orbital Velocity in the X_o Direction at the R^{th} Fin and the i^{th} Wave
$\dot{\zeta}_{Z_{OBM_i}}(t)$	Wave Orbital Velocity in the Z_o Direction at the M^{th} Hull Section and for the i^{th} Wave
$\dot{\zeta}_{Z_{OFR_i}}(t)$	Wave Orbital Velocity in the Z_o Direction at the R^{th} Fin and the i^{th} Wave
$[\overline{\alpha}(\omega)]$	A Weighting Matrix
$[\overline{\beta}(\omega)]$	A Weighting Matrix

ABSTRACT

The development of a nonlinear frequency domain simulation which accomodates frequency independent nonlinearities is described. Although developed around the dynamics of a particular naval craft, the simulation can be applied to a general situation and need not be restricted solely to the prediction of ship motions. The workability and usefulness of the simulation is demonstrated by simulating three scenarios with the SWATH 6A craft. Two scenarios are open loop; the third includes automatic control. These scenarios are also simulated in the time domain using a generalized nonlinear time domain simulation which is based on the same modeling of the craft dynamics as that which is used for the nonlinear frequency domain simulation. The results obtained with these simulations agree for each of the scenarios simulated.

When the results obtained with the nonlinear frequency domain simulation are contrasted with those obtained with a linear frequency domain simulation which employs equivalent linearization for the handling of nonlinearities, a lack of agreement becomes noticeable. This highlights a limited usefulness of equivalent linearization.

ADMINISTRATIVE INFORMATION

This work has been jointly funded by the General Hydromechanics Research Program Task Area SR0230101, element number 61153N, work unit 1572-145, and by the Ships, Subs, and Boats Program, Task Area ZF43-421. The latter funding was authorized by the Naval Material Command (08T) and administered by the Ship Performance Department High Performance Vehicles Program (1507).

INTRODUCTION

Frequency domain analysis is extremely useful in the study of dynamic systems. When it is known that a system is dominated by linear dynamics, frequency domain techniques can be applied in a rather casual and routine manner. This situation changes when the system exhibits nonlinearities which cannot be ignored. Very often, when nonlinearities must

be recognized, some form of linearization is attempted or the frequency domain approach is abandoned altogether. This can be unfortunate since linearization is not always carried out appropriately (in which case misleading results are obtained), and abandoning the frequency domain approach means relinquishing a very powerful tool.

This report describes a technique which does not force a choice of either alternative. The technique is an iterative process in the frequency domain which will accommodate single valued nonlinearities. It was developed around the dynamics of the SWATH 6A, a Small-Waterplane-Area-Twin-Hull craft. However, it can be applied to any situation in which nonlinearities are significant and must be accounted for in the analysis.

COORDINATE SYSTEM

Only heave and pitch are treated in this report. Nothing is lost by this restriction except unnecessary complication since, in the conventional modeling, the combination, sway-yaw-roll, is assumed to be uncoupled from the combination, pitch-heave, and further, surge is assumed to be uncoupled from any other degree of freedom*.

Motions and forces are referenced to a frame that is a right-handed orthogonal Cartesian coordinate system. This frame does not rotate but translates with constant velocity, U_o, and, thus, is an inertial frame.

The velocity, U_o, is the mean forward velocity of the craft. The origin of this frame lies in the plane of the mean free surface and the plane of the mean position of the longitudinal centerplane of the craft.

*It must be emphasized that the technique described in this report can be applied to a six-degree-of-freedom coupled system. The modeling chosen for demonstrating the technique just happens, by convention, to be a rather highly decoupled system.

The $X_o O_o Y_o$ plane coincides with the plane of the mean free surface; the X_o-axis points toward the bow of the craft; the Y_o-axis points toward port; and the Z_o-axis points up. The craft makes small motions (i.e., perturbations) about this coordinate system. The reference point on the craft is that point which, at calm water equilibrium, coincides with the origin of the coordinate system.

SWATH CRAFT SYSTEM DYNAMICS MODELING

A system modeling that is employed for predicting surface ship motions and one that is used at the David W. Taylor Naval Ship Research and Development Center (DTNSRDC) for predicting motions of SWATH craft consists of a set of equations usually referred to as differential equations with frequency dependent coefficients. Considering the vertical plane only, the steady state equaiion of heave is:

$$(M+A_{33})\ddot{Z}_o+B_{33}\dot{Z}_o+C_{33}Z_o+A_{35}\ddot{\theta}+B_{35}\dot{\theta}+C_{35}\theta = \bar{F}e^{-j\omega t} * \qquad (1)$$

The equation for pitch is:

$$(I_5+A_{55})\ddot{\theta}+B_{55}\dot{\theta}+C_{55}\theta+A_{53}\ddot{Z}_o+B_{53}\dot{Z}_o+C_{53}Z_o = \bar{T}e^{-j\omega t} \qquad (2)$$

In the use of equations (1) and (2), it is assumed that the steady state can be reached. $(M + A_{33})$, B_{33}, A_{35}, B_{35}, $(I_5 + A_{55})$, B_{55}, A_{53} and B_{53} are functions of frequency. C_{33}, C_{35}, C_{55} and C_{53} are frequency

---

* The bar over a symbol indicates a complex quantity. Also only the real part of the forcing function is assumed.

independent. The amplitudes, $\bar{F}$ and $\bar{T}$, of the forcing functions are complex to allow for phase relationships with respect to the corresponding wave. Since the equations (1) and (2) are linear steady state equations, they generate sinusoidal responses to sinusoidal inputs; i.e.,

$$Z_o(t) = \bar{Z}_{oa} e^{-j\omega t}* \tag{3}$$

$$\theta(t) = \bar{\theta}_a e^{-j\omega t} \tag{4}$$

Both $\bar{Z}_{oa}$ and $\bar{\theta}_a$ are complex to allow for phase relationships with respect to the forcing functions. Substitution of (3) and (4) into (1) and (2), gives the following:

$$\bar{Z}_{oa} = \bar{H}_{33}(\omega)\bar{F} + \bar{H}_{35}(\omega)\bar{T} \tag{5}$$

$$\bar{\theta}_a = \bar{H}_{53}(\omega)\bar{F} + \bar{H}_{55}(\omega)\bar{T} \tag{6}$$

Here

$$\bar{H}_{33}(\omega) = \bar{K}_4/\bar{K}_o \tag{7}$$

$$\bar{H}_{35}(\omega) = -\bar{K}_2/\bar{K}_o \tag{8}$$

$$\bar{H}_{53}(\omega) = -\bar{K}_3/\bar{K}_o \tag{9}$$

$$\bar{H}_{55}(\omega) = \bar{K}_1/\bar{K}_o \tag{10}$$

and

$$\bar{K}_1(\omega) = -\omega^2(M + A_{33}) - j\omega B_{33} + C_{33} \tag{11}$$

$$\bar{K}_2(\omega) = -\omega^2 A_{35} - j\omega B_{35} + C_{35} \tag{12}$$

$$\bar{K}_3(\omega) = -\omega^2 A_{53} - j\omega B_{53} + C_{53} \tag{13}$$

$$\bar{K}_4(\omega) = -\omega^2(I_5 + A_{55}) - j\omega B_{55} + C_{55} \tag{14}$$

$$\bar{K}_o = \begin{vmatrix} \bar{K}_1(\omega) & \bar{K}_2(\omega) \\ \bar{K}_3(\omega) & \bar{K}_4(\omega) \end{vmatrix} \tag{15}$$

*Only the real parts of the responses are assumed.

For a particular wave frequency both $\overline{F}(\omega)$ and $\overline{T}(\omega)$, the amplitudes of the wave induced exciting force and moment associated with this wave, are known and the responses $\overline{Z}_{oa}(\omega)$ and $\overline{\theta}_a(\omega)$ are easily computed. Of course, this can be done for any sum of a finite number of frequencies by computing the response to each frequency and summing the responses. This is what is meant by a linear system.

FREQUENCY INDEPENDENT NONLINEARITIES

A next level of complexity when considering frequency domain analysis results from the introduction of frequency independent single valued nonlinearities. If a linear frequency domain analysis is to be used, some type of linearization must be carried out. Reference 1 includes a discussion of the application of equivalent linearization to the same problem selected for demonstrating the nonlinear frequency domain simulation described in this report. If the system is weakly nonlinear such that the output associated with any single frequency input can be approximated by a sinusoid of the same frequency and if its amplitude is adjusted to a best least squares fit to the nonlinear response, the application of equivalent linearization is valid. However, when the input, as is often the case in ship design problems, is a seaway represented by a sum of a finite number of sinusoids of differing frequency, and the nonlinearity involved is associated with, for example, the square of the sum of these sinusoids the use of equivalent linearization may be inappropriate.

NONLINEARITIES MODELED IN SWATH 6A SIMULATIONS

The nonlinearities that are incorporated in SWATH ship modeling,

as given by Lee[1]*, are frequency independent and single valued. They are the viscous lift and drag on the hull sections and fins. For the M^{th} hull section (see Figure 1) the viscous lift and drag are given by

$$L_{BM} = \frac{1}{2} \rho V_{BM}^2 A_{PBM} a_o \sin\alpha_{BM} |\cos\alpha_{BM}| \quad (16)$$

$$D_{BM} = \frac{1}{2} \rho V_{BM}^2 A_{PBM} C_{DBM} \sin\alpha_{BM} |\sin\alpha_{BM}| \quad (17)$$

Where

A_{PBM} = the projected area of the M^{th} hull section (m^2)

ρ = the mass density of seawater (1031.9 Kg/m^3)

a_o = 0.07

C_{DBM} = the crossflow drag coefficient at the M^{th} hull section (=0.5 for all sections)

V_{BM} = the total relative velocity between the craft and the water at the M^{th} hull section (m/sec)

α_{BM} = the angle of attack of the flow at the M^{th} hull section

$$V_1 = -U_o \cos\theta + \dot{Z}_o \sin\epsilon - \Sigma_i \dot{\zeta}_{Z_{OBM}}(i) \sin\theta + \Sigma_i \dot{\zeta}_{X_{OBM}}(i) \cos\theta \quad (18)$$

$$V_2 = -U_o \sin\theta - \dot{Z}_o \cos\epsilon + X_{OBM}\dot{\theta} + \Sigma_i \dot{\zeta}_{Z_{OBM}}(i) \cos\theta + \Sigma_i \dot{\zeta}_{X_{OBM}}(i) \sin\theta \quad (19)$$

$$V_{BM}^2 = V_1^2 + V_2^2 \quad (20)$$

$$\alpha_{BM} = \tan^{-1} V^2/V^1 \quad (21)$$

Here $\dot{\zeta}_{Z_{OBM}}(i)$ and $\dot{\zeta}_{X_{OBM}}(i)$ are the vertical and longitudinal components, respectively, of the wave orbital velocity at the M^{th} hull section and for the i^{th} wave component. X_{OBM} is the x-coordinate of the location of the M^{th} body section. U_o is the constant forward speed of the craft. The viscous lift and drag at the R^{th} fin (there are four fins) are given by

$$L_{FR} = \frac{1}{2} \rho V_{FR}^2 A_{FR} C_{LFR\alpha} \sin\alpha_{FR} \quad (22)$$

$$D_{FR} = \frac{1}{2} \rho A_{FR} C_{DFR} V_{FR}^2 \sin\alpha_{FR} |\sin\alpha_{FR}| \quad (23)$$

---

*References listed on Page 27.

Where

$$V_3 = -U_o \cos\theta + \dot{Z}_o \sin\theta - \sum_i \dot{\zeta}_{Z_{OFR}}(i) \sin\theta + \sum_i \dot{\zeta}_{X_{OFR}}(i) \cos\theta \quad (24)$$

$$V_4 = -U_o \sin\theta - \dot{Z}_o \cos\theta + X_{OFR}\dot{\theta} + \sum_i \dot{\zeta}_{Z_{OFR}}(i) \cos\theta + \sum_i \dot{\zeta}_{X_{OFR}}(i) \sin\theta \quad (25)$$

$$V_{FR}^2 = V_3^2 + V_4^2 \quad (26)$$

$$\alpha_{FR} = \tan^{-1} V_3/V_4 \quad (27)$$

here $\dot{\zeta}_{Z_{OFR}}(i)$ and $\dot{\zeta}_{X_{OFR}}(i)$ are the vertical and longitudinal components respectively, of the wave orbital velocity at the R^{th} fin and for the i^{th} wave component. X_{OFR} is the x-coordinate of the R^{th} fin. U_o is the constant forward speed of the craft. For the SWATH 6A

C_{LFR_α} = 4.38 for the two forward fins and 3.4 for the two aft fins

C_{DFR} = 1.2 for all fins

A_{FR} = 8.05 m^2 (for R=1, the area of the forward port fin)

= 8.05 m^2 (for R=2, the area of the forward starboard fin)

A_{FR} = 24.03 m^2 (for R=3, the area of the aft starboard fin)

= 24.03 m^2 (for R=4, the area of the aft port fin)

In addition to the nonlinearities identified above, there are nonlinearities associated with the modeling of an active controller. Figure 2 shows a flowchart for the implementation of the controller algorithm. The fin order is proportional to heave velocity, $\dot{Z}_0(t)$, where the constant of proportionality, γ, has the value 3.048^o/m sec^{-1}. The fin angle, δ, is positive for trailing edge up. The order is clipped at $\delta_{MAX} = 15^o$ and passed through a first order lag. This equation is implemented using Tustin's[4] method. The explicit implementation is shown in BLOCK 4 of Figure 2. The rate at which the fin moves is limited if necessary, to $\dot{\delta}_{MAX} = 10^o$/sec. In the implementing of the controller, clipping and rate limiting can, of course, be strong nonlinearities.

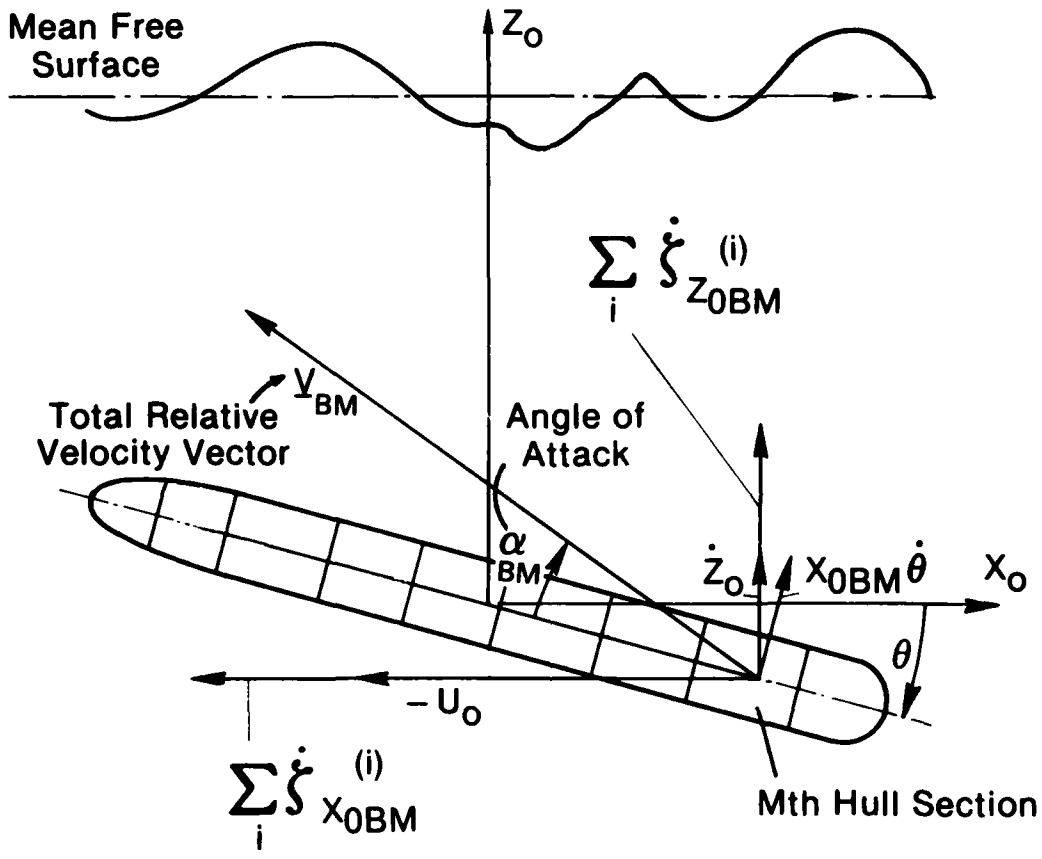

Figure 1 - Velocity Vector Involved in Computing Viscous Lift and Drag

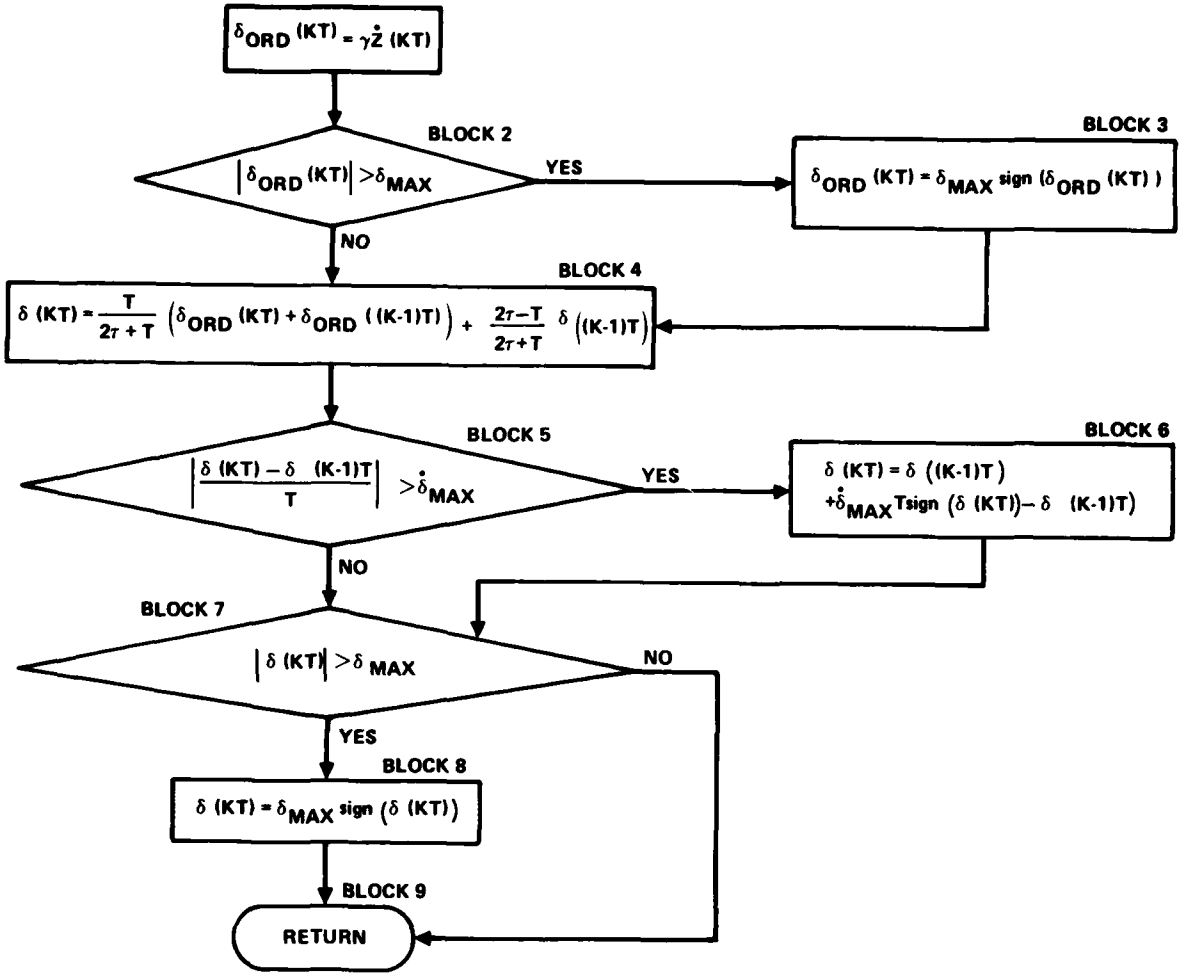

Figure 2 - Flowchart for the Fin Angle Controller

NONLINEAR FREQUENCY DOMAIN SIMULATION

The overview of the nonlinear frequency domain simulation given below is followed by a detailed description.

What is required is a solution to the vector equation

$$\underline{\bar{X}}(\omega) = \left[\bar{H}(\omega)\right] (\underline{\bar{F}}_{EXT}(\omega)+\underline{\bar{F}}_{NL}(\omega)) \tag{28}$$

Here

$$\underline{\bar{X}}(\omega) = \{\bar{Z}_{oa}(\omega)\ \bar{\theta}_a(\omega)\}^T \tag{29}$$

$$\left[\bar{H}(\omega)\right] = \begin{matrix} \bar{H}_{33}(\omega) & \bar{H}_{35}(\omega) \\ \bar{H}_{53}(\omega) & \bar{H}_{55}(\omega) \end{matrix} \tag{30}$$

$$\underline{\bar{F}}_{EXT}(\omega) = \{\bar{F}(\omega)_{EXT}\ \bar{T}(\omega)_{EXT}\}^T \tag{31}$$

$$\underline{\bar{F}}_{NL}(\omega) = \{\bar{F}(\omega)_{NL}\ \bar{T}(\omega)_{NL}\}^T \tag{32}$$

Here $\underline{\bar{F}}_{EXT}(\omega)$ is the complex frequency spectrum of wave induced hydrodynamic forces and moments, which are independent of ship motions, combined with all other applied forces and moments. $\underline{\bar{F}}_{NL}(\omega)$ is the complex frequency spectrum of all frequency independent nonlinear forces and moments. Among these are the lift and drag on the hulls and fins as well as nonlinear forces and moments associated with active control. $\underline{\bar{F}}_{NL}(\omega)$ cannot be obtained by a direct frequency domain operation. It can, however, be obtained from a time domain computation of the nonlinear forces and moments and a transformation, via an FFT, to the complex frequency domain. Initially, the craft is assumed to have no motion except for a constant forward speed. Having applied $\underline{\bar{F}}_{EXT}(\omega)$ only($\underline{\bar{F}}_{NL}(\omega)$ is set to zero at this point) one has a motion vector $\underline{\bar{X}}(\omega)$. This motion vector is transformed via FFT^{-1} to its time domain equivalent to obtain $\underline{X}(t)$. One can now carry

*The under bar indicates a vector.

out all motion dependent nonlinear force and moment computations including those contributed by active control. The forces and moments obtained are passed through an FFT and one obtains $\overline{F}_{NL}(\omega)$, say, at the N^{th} iteration. One now computes the motion vector at the $(N+1)^{th}$ iteration as follows:

$$\overline{X}(\omega)^{N+1} = [\overline{H}(\omega)](\overline{F}_{EXT}(\omega) + \overline{F}_{NL}(\omega)^{N})^{*} \tag{33}$$

The iterative process is continued until convergence is achieved. In choosing a discrete frequency domain representation, the frequency spacing, $\Delta\omega$, is selected to insure a fundamental period ($T_{max} = 2\pi/\Delta\omega$) in the time domain large enough to be a representative portion of the response to a stationary random input. Also, the highest frequency represented ($\omega_{max} = (N-1)\Delta\omega$) should be at least twice the highest frequency at which significant response is expected.

Figure 3 shows a flowchart for the nonlinear frequency domain simulation. The simulation starts with an initialization block (not shown) in which a sine wave approximation to the seaway and the wave induced forces and moment are computed. These are motion independent forces and moments which are combined with all other applied forces and moments. The sum is labelled $\overline{F}_{EXT}(\omega)$. Wave orbital velocities are also computed here, the state vector, $\underline{X}(t) = \{Z_0(t)\ \theta\ (t)\}^T$ is set to zero $\overline{F}_{OLD}(\omega)$ is set to zero as is the state vector, $\overline{X}_0(\omega)$. Nonlinear forces and moments which can, of course, include linear terms, are computed in BLOCK I in the time domain for one cycle of the lowest non-zero frequency used in the frequency domain representation of the system. BLOCK II transforms the nonlinear forces and moments to their frequency domain description via a Fast Fourier Transform (FFT). These are added, in BLOCK III, to $\overline{F}_{EXT}(\omega)$. This sum gives a

*In the actual implementation of the algorithm $\overline{F}_{NL}(\omega)^{N}$ is modified to increase the region of convergence.

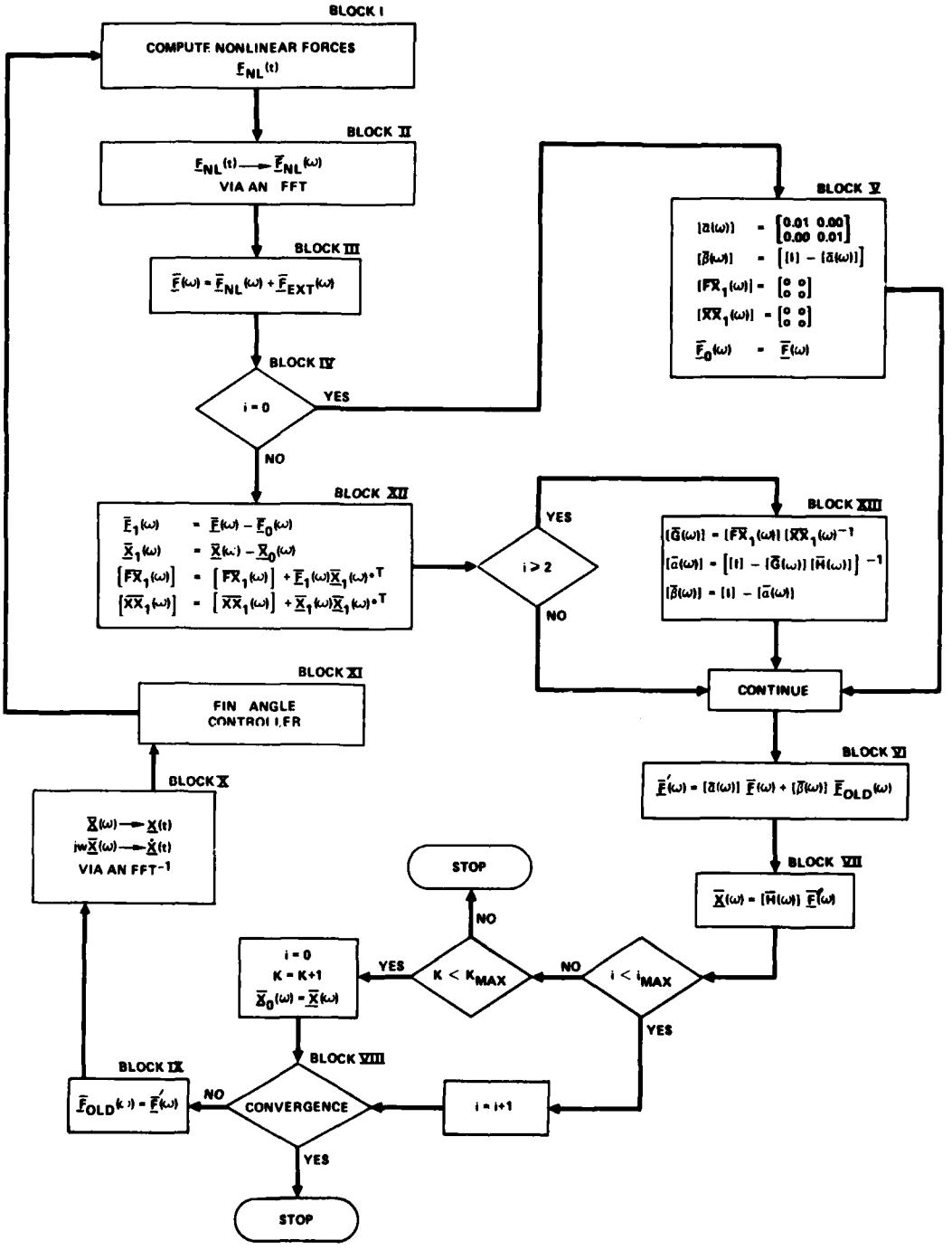

Figure 3 - Flowchart for the Nonlinear Frequency Domain Simulation

frequency domain description of the total forces and moments, $\underline{\bar{F}}(\omega)$ acting on the craft. For the first iteration, i=o, BLOCK V comes into play, the matrices, $\left[\bar{\alpha}(\omega)\right]$, $\left[\bar{\beta}(\omega)\right]$, and $\left[\bar{G}(\omega)\right]$ are initialized and $\underline{\bar{F}}_0(\omega)$, is set equal to the recently computed $\underline{\bar{F}}(\omega)$ and saved. In BLOCK VI, $\underline{\bar{F}}'(\omega)$, the input to the system transfer matrix, $\left[\bar{H}(\omega)\right]$, is computed. This computation is the actual force acting on the system only when convergence has been achieved. The state vector, $\underline{\bar{X}}(\omega)$, in the frequency domain is computed in BLOCK VII. The simulation has two loops, an inner loop over the index i and an outer loop over the index k. If during any iteration the convergence criteria in BLOCK VIII are met, the simulation stops. If not, $\underline{\bar{F}}_{OLD}(\omega)$ is set equal to the last value of $\underline{\bar{F}}'(\omega)$. $\underline{\bar{X}}(\omega)$ and $j\omega\underline{\bar{X}}(\omega)$ are transformed to their time domain description via an FFT^{-1} in BLOCK X. When i equals i_{MAX}, the k-loop is activated, i is reset to zero, k is set to k+1, and $\underline{\bar{X}}_0(\omega)$ is replaced with the latest values of $\underline{\bar{X}}(\omega)$. This has the effect of restarting the iteration process with the old values of $\underline{\bar{X}}_0(\omega)$ and $\underline{\bar{F}}_0(\omega)$ updated. This very important updating was found to speed up convergence significantly. The simulation continues as before. If i=0 BLOCK XII is activated. Computations carried out in BLOCK XII and BLOCK XIII lead to the computation in BLOCK VI, of $\underline{\bar{F}}'(\omega)$. Following BLOCK XIII, the simulation continues as before.

SCENARIOS SIMULATED

Three scenarios were simulated to demonstrate applications of the nonlinear frequency domain simulation. In the first scenario, the SWATH 6A is proceeding at, nominally, equilibrium depth and at a speed of 10 knots into a head sea state 6. The seaway is modeled by a Pierson-Moskowitz energy spectrum which in turn is approximated by 15 sine waves

in random phase to one another. The modeling of the seaway is discussed in Appendix A. A second scenario is the same as the first except an active controller has been added. A third scenario is a repeat of the first for zero speed. For the third scenario the seaway is approximated by 12 sine waves in random phase to one another.

The output from the simulations is obtained using three different appoaches. One approach uses the technique described in this report; the second approach uses equivalent linearization and a linear frequency domain simulation; and the third approach uses a generalized time domain simulation which does not require a linearization of the nonlinearities. The second scenario was not simulated with the linear frequency domain simulation since that simulation will not accommodate active controllers.

PRESENTATION OF RESULTS

The results presented here and obtained using the nonlinear frequency domain simulation technique are discussed in relation to, and are compared with, results obtained with a Generalized Nonlinear Time Domain Motion Predictor for SWATH Craft (Reference 2) and with the Mono-Hull or Twin-Hull Ship Motion Predictions Computer Program (Reference 3). In the former, the full power of the nonlinearities is modeled as it is in the Nonlinear Frequency Domain Simulation, and consequently, the steady state solutions obtained should agree with solutions obtained with the Nonlinear Frequency Domain Simulation*. The results obtained with the program of Reference 3 do not agree since this program treats the nonlinearities via equivalent linearization and one cannot expect agreement.

*Only steady state solutions can be obtained with the Nonlinear Frequency Domain Simulation.

Figures 4, 5, 6, and 7 show results obtained when the three simulations carry out scenarios 1 and 2. Figure 4 shows the heave response, Figure 5 the heave phase, Figure 6 the pitch response, and Figure 7 the pitch phase. In all these figures, the responses obtained with the Nonlinear Frequency Domain Simulation agree with those obtained with the Generalized Nonlinear Time Domain Motion Predictor while the results obtained with the linearized frequency domain simulation do not agree with the other two over the full frequency span. It is important to observe that in Figures 4 and 6 both the Nonlinear Frequency Domain Simulation and the Generalized Nonlinear Time Domain Motion Predictor show motion amplitudes at frequencies lower than 0.45 rad/sec, the lowest frequency wave input. Of course, the linearized frequency domain cannot and does not predict such motions. Since the phase plots, Figures 5 and 7, show phases relative to the input wave there can be no entires on these figures for frequencies lower than 0.45 rad, the frequency of the longest wave input.

Figures 8, 9, 10, and 11 show results obtained when the three simulations carry out scenario 3. Since the forward speed for this scenario is zero, no results with a controller are included. At zero speed, the fins are not force effectors. Again, the results obtained with the nonlinear frequency domain simulation and the generalized time domain simulation are in agreement and, again, motion is predicted at frequencies lower than the lowest frequency wave input. The results obtained with the linear frequency domain simulation are not in agreement. In fact, here the disagreement is more significant than that of scenario 1. In scenario 1, the disagreement at heave resonance is approximately 11% whereas in scenario 3 the disagreement is approximately 35%.

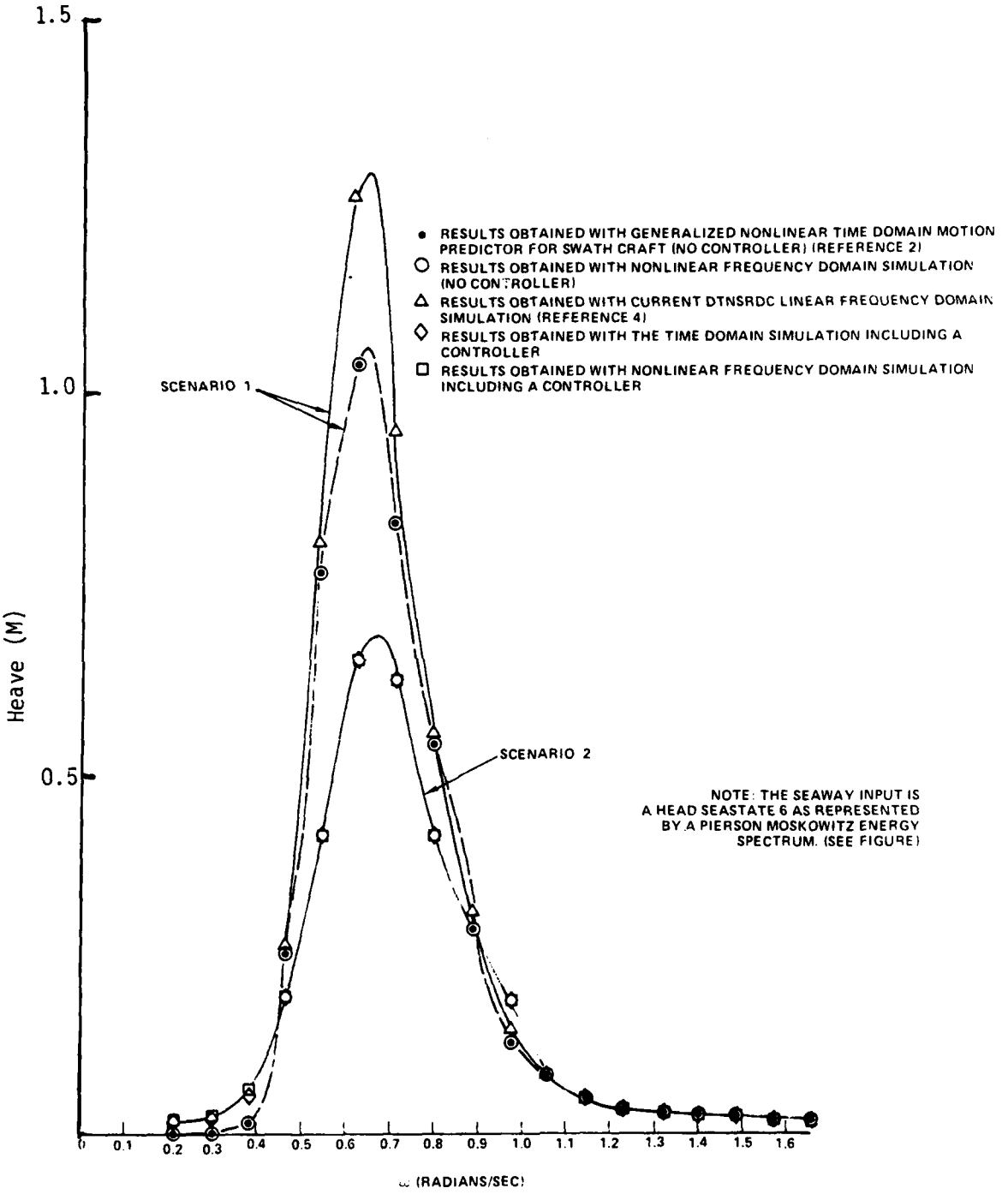

Figure 4 - Heave Amplitude for Scenarios 1 and 2

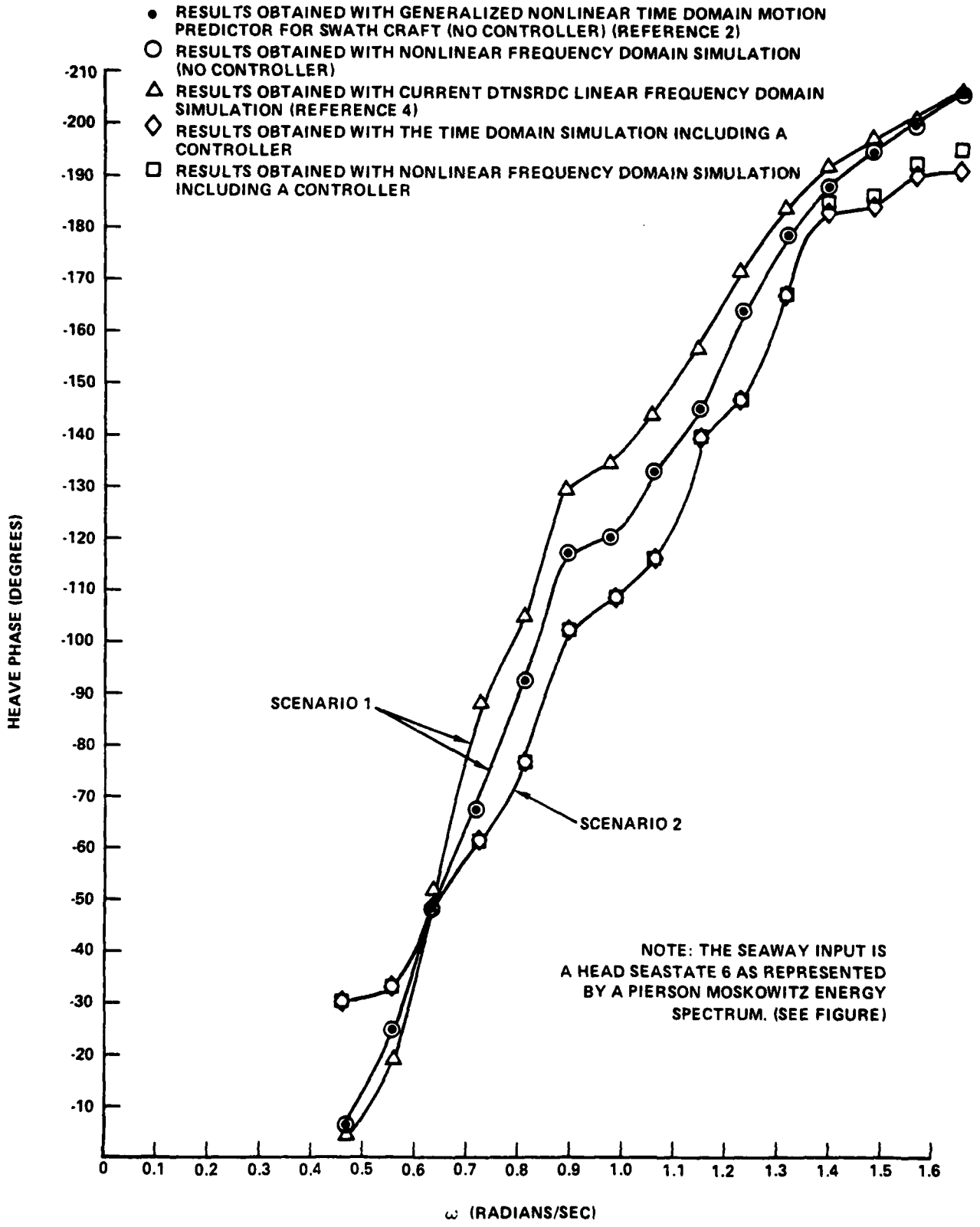

Figure 5 - Heave Phase for Scenarios 1 and 2

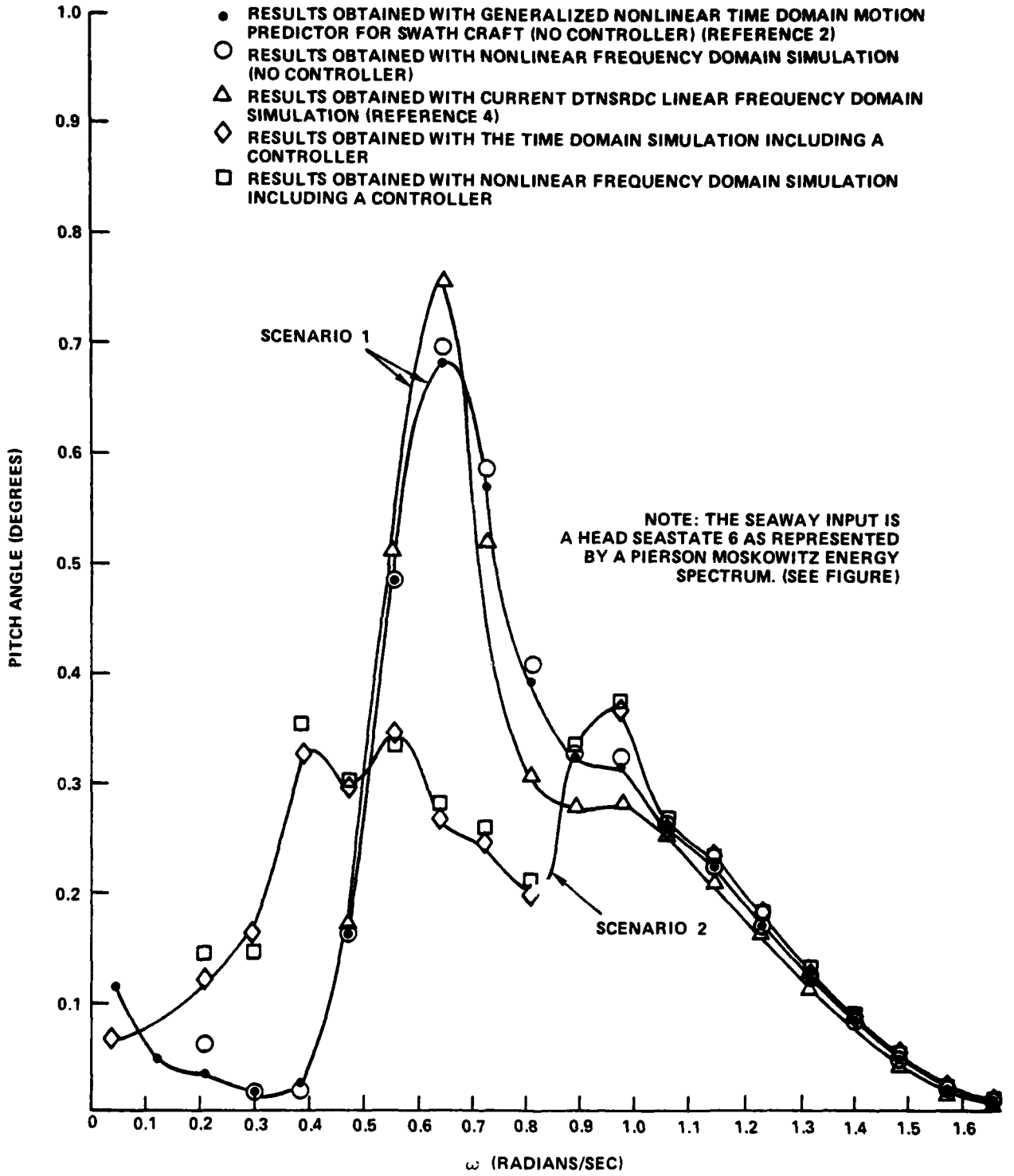

Figure 6 - Pitch Angle Amplitude for Scenarios 1 and 2

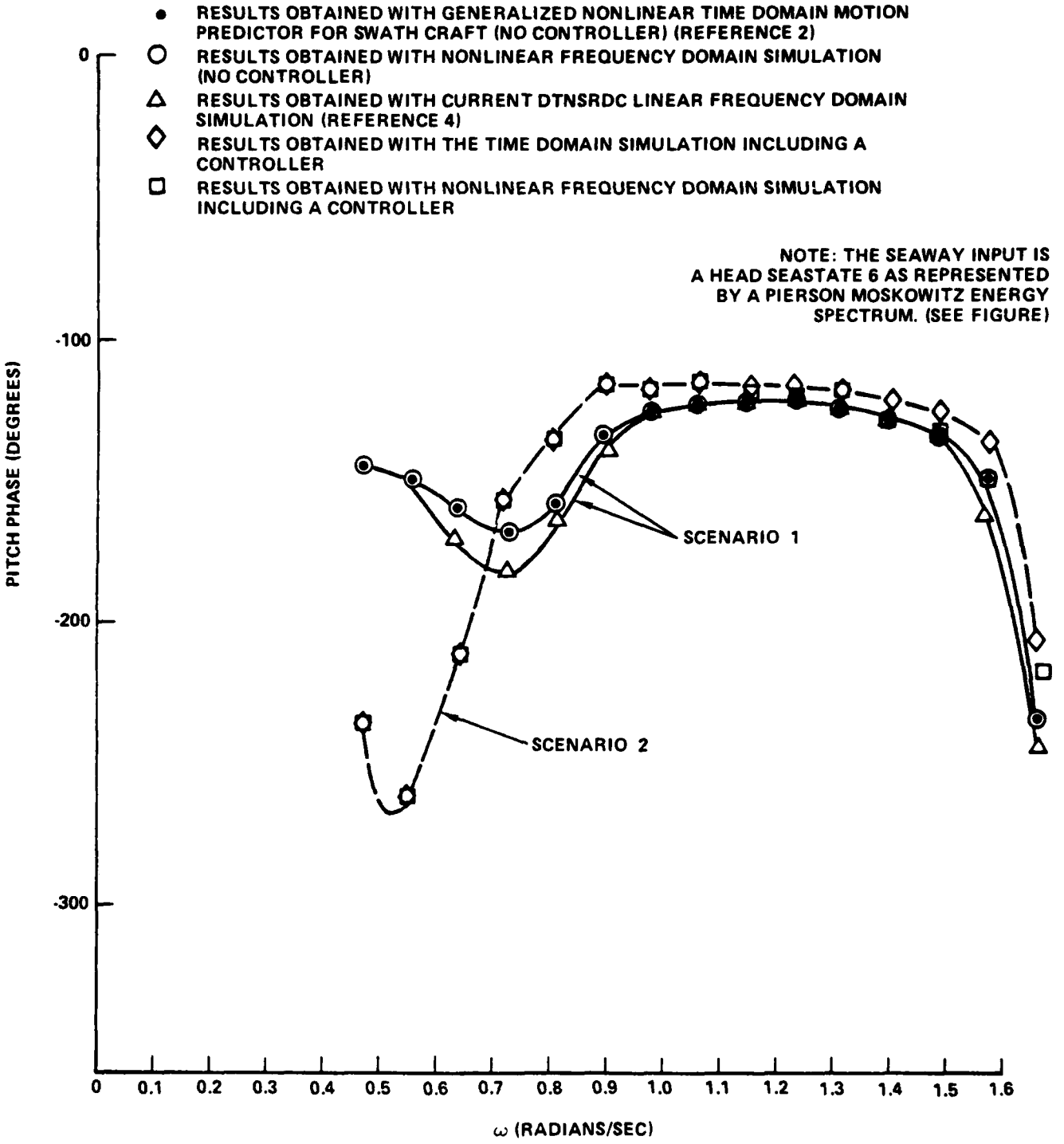

Figure 7 - Pitch Angle phase for Scenarios 1 and 2

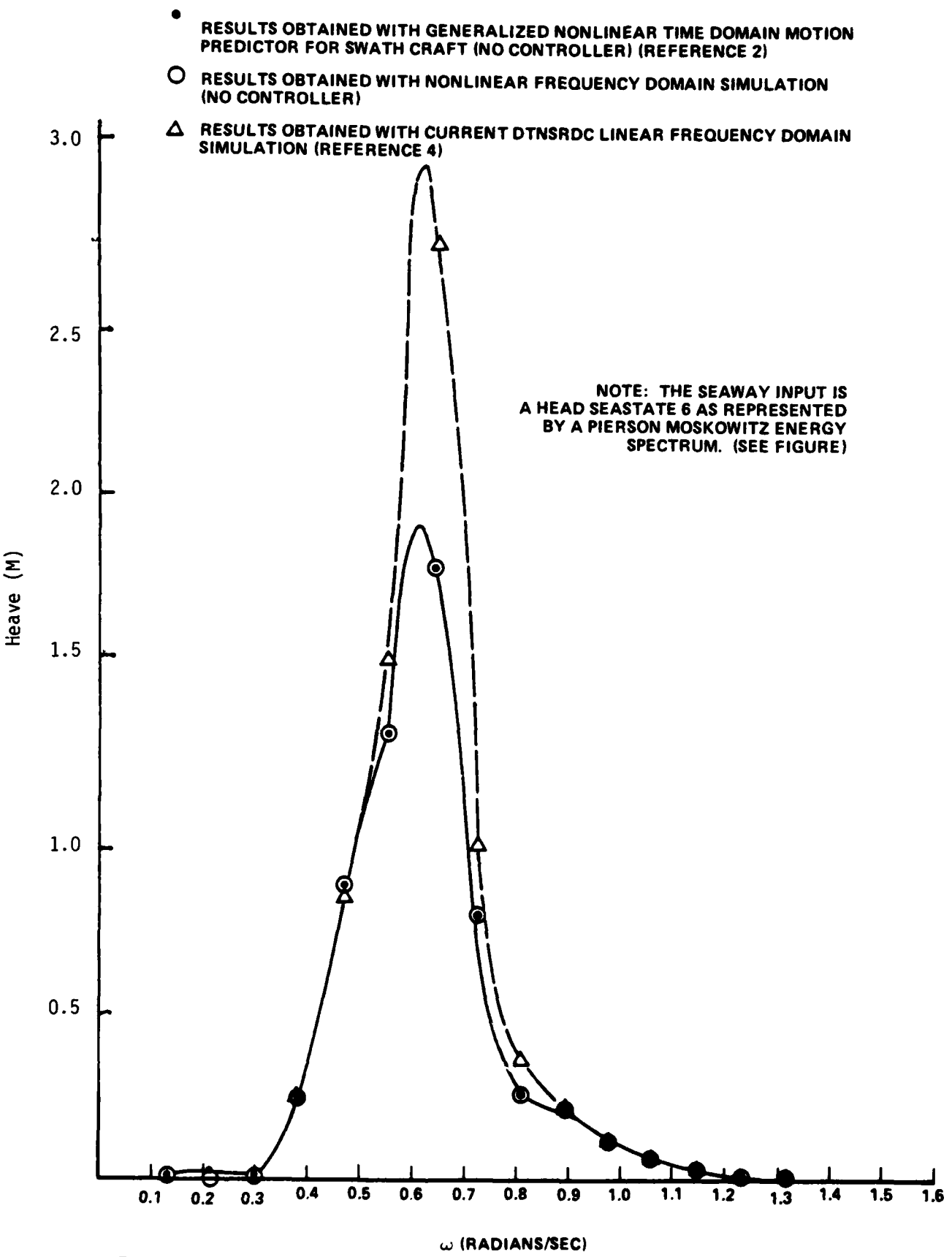

Figure 8 - Heave Amplitude for Scenario 3

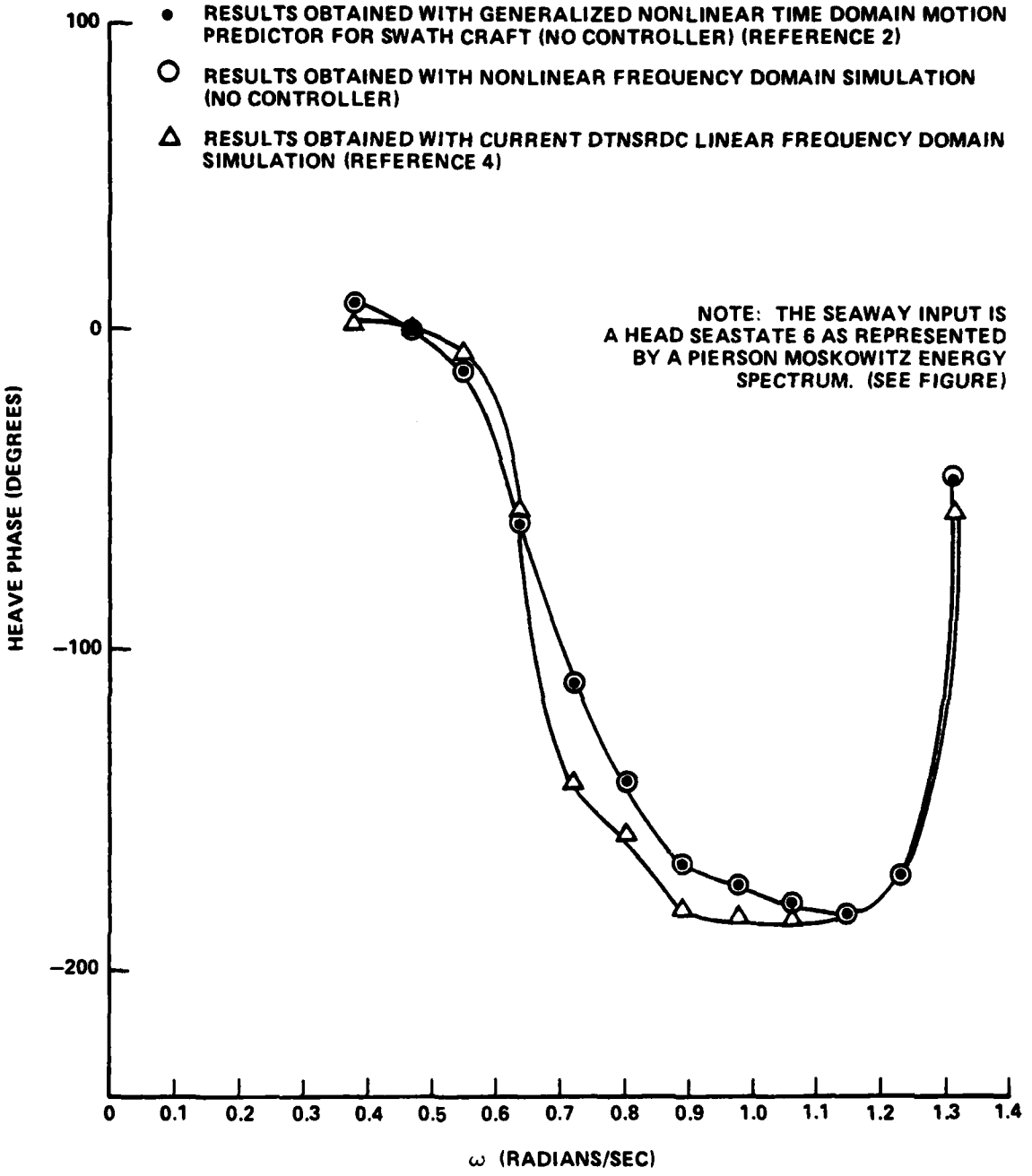

Figure 9 - Heave Phase for Scenario 3

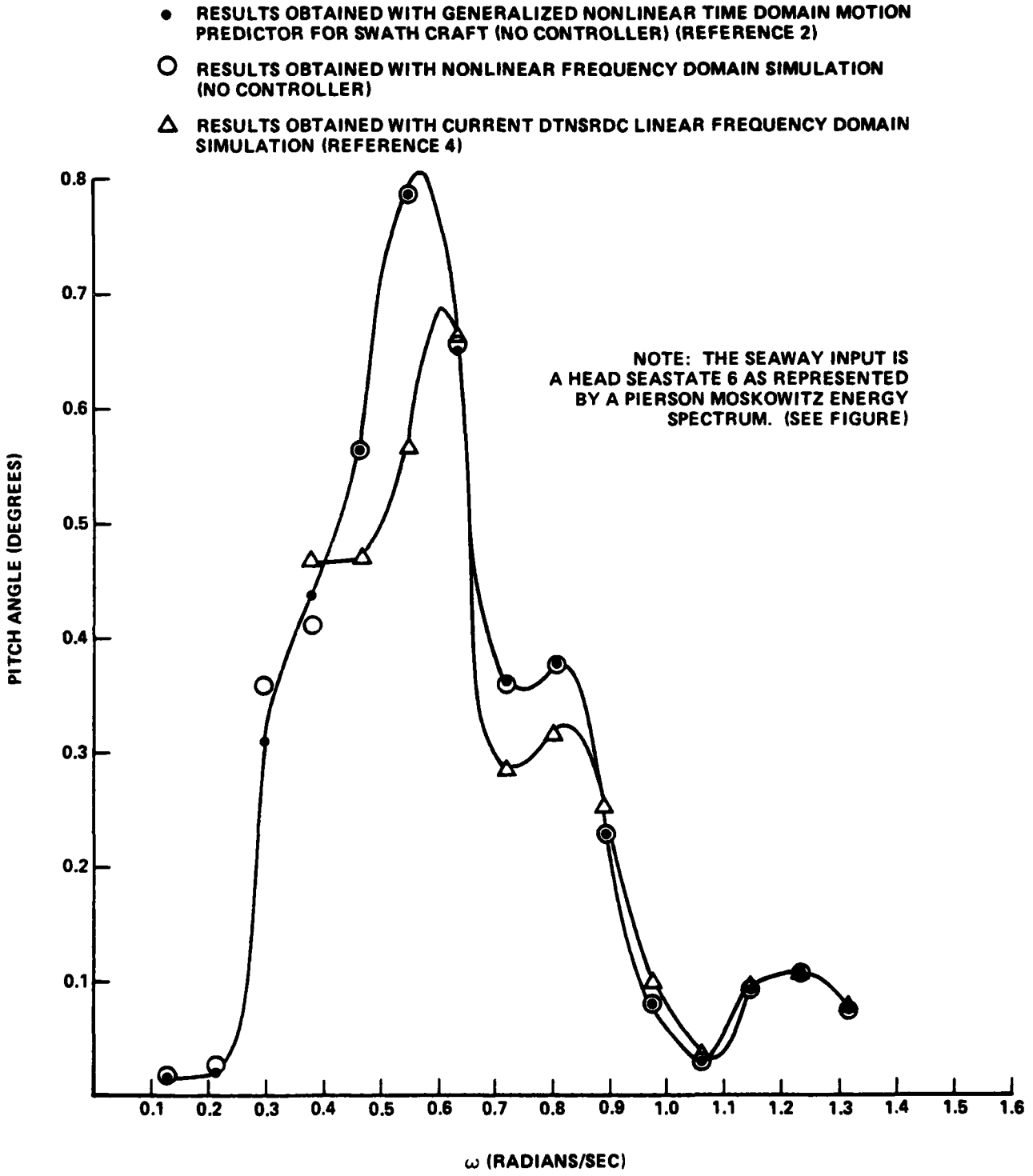

Figure 10 - Pitch Angle Amplitude for Scenario 3

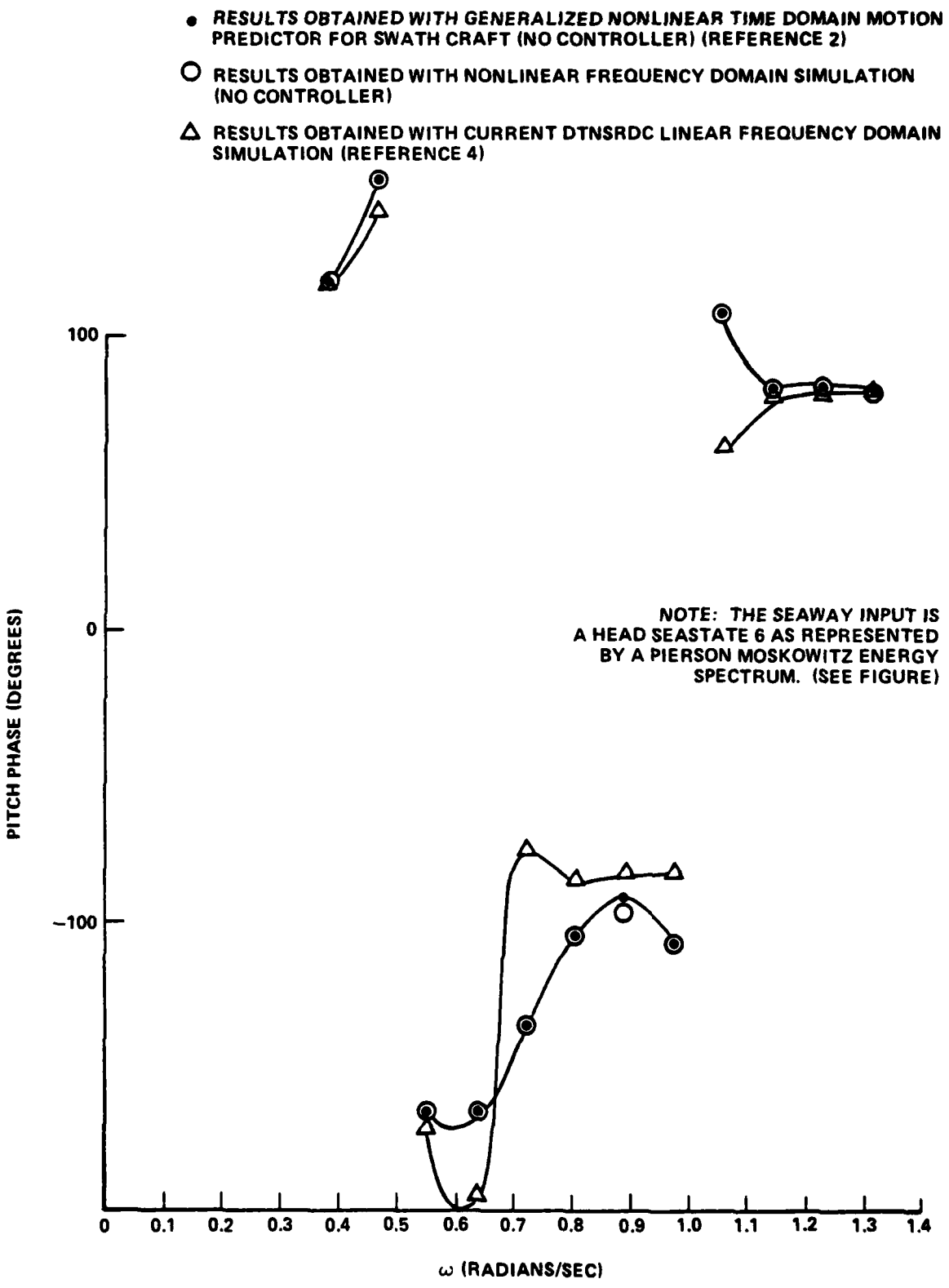

Figure 11 - Pitch Phase Angle for Scenario 3

Figure 12 shows a time history of one cycle of fin order and fin displacement under automatic control. Figure 13 shows a time history of one cycle of heave displacement with and without automatic control.

CONCLUSIONS

The technique developed in this report for handling frequency independent nonlinearities in frequency domain analysis is shown, by example, to be a viable technique. The question as to the range of nonlinear mathematics throughout which the technique can be successfully applied has not been answered. This is an important question. However, the answer to this question requires further effort.

ACKNOWLEDGMENT

Under Contract Purchase Order No. N00167-78-M-3869, Mr. David Newman of ORI, Inc., Silver Spring, Maryland, developed the convergence scheme used in the technique described in this report and also designed and developed the computer programs required in order to carry out the reported effort.

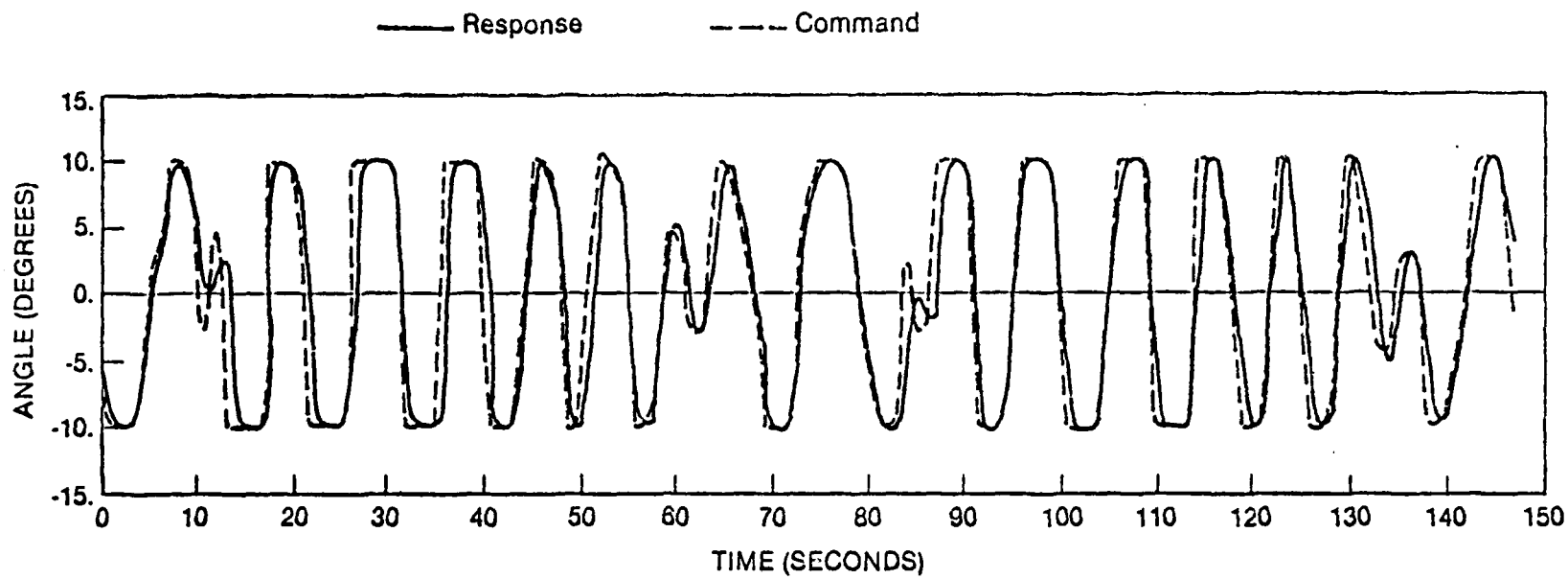

Figure 12 - Time History of One Cycle of Fin Order and Fin Displacement under Automatic Control

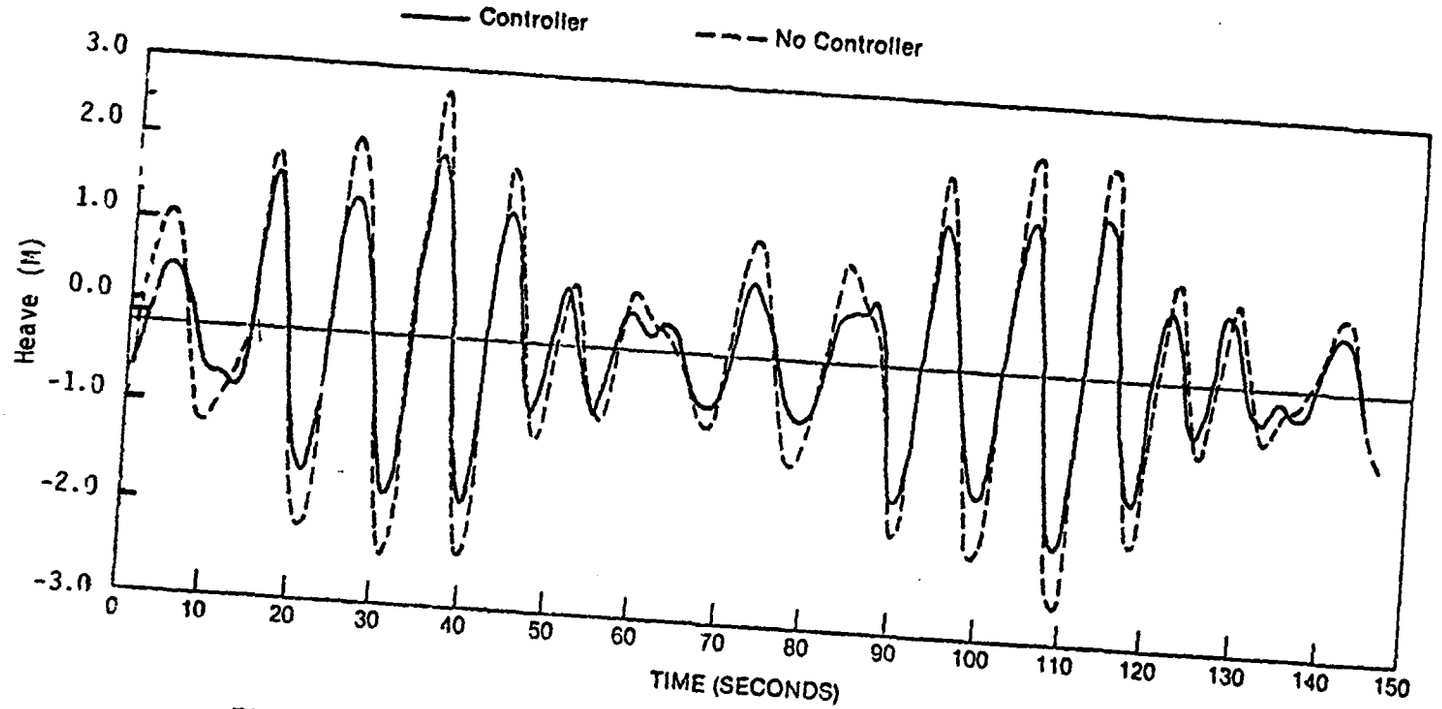

Figure 13 - Time History of One Cycle of Heave Displacement with and without Controller

REFERENCES

1. Lee, C.M., "Theoretical Prediction of Motion of Small-Waterplane-Area-Twin-Hull (SWATH) Ships in Waves," DTNSRDC Report 76-0046 (1976).

2. Livingston, Walter, "Generalized Non-Linear Time Domain Motion Predictor for SWATH Craft," DTNSRDC/SPD-0857-01 (July 1978).

3. McCreight, K.K. and C.M. Lee, "Manual for Mono-Hull or Twin-Hull Ship Motion Predictions Computer Program," DTNSRDC Report SPD-676-02 (1972).

4. Cadzow, J.A., "Discrete Time Systems," Prentice-Hall (1976).

APPENDIX A

SEAWAY DESCRIPTION

SEAWAY DESCRIPTION

The time history of the surface elevation of a seaway is usually approximated, in digital simulations, by a finite sum of sine waves. In this report, the Pierson-Moskovitz representation of the seaway is used. The formula is

$$P(\omega) = \frac{.77898}{\omega^5} e^{-\frac{97715.0}{(V_w \cdot \omega)^4}}$$

where

$P(\omega)$ is the energy ordinate at frequency ω in meters

ω is the frequency in rad/sec

V_w is the wind speed in knots = $18.82 \times \sqrt{H_{1/3}/2}$

$H_{1/3}$ is the significant waveheight in meters

A plot of this spectrum for a Sea State 6 (significant waveheight of 4.57 m is shown in Figure 14 for a ship moving at 10 knots into a head sea and 0 knots into a head sea.

Twelve sine waves were chosen to approximate the seaway for the 0 knot case while 15 sine waves were used in the encounter frequency domain for a ship moving into a head sea at 10 knots. For the former, the 12 sine waves are:

$.232\sin(0.3825t + \Omega_1)$	$.884\sin(0.7255t + \Omega_5)$	$.418\sin(1.0615t + \Omega_9)$
$.722\sin(0.4675t + \Omega_2)$	$.695\sin(0.8075t + \Omega_6)$	$.351\sin(1.1476t + \Omega_{10})$
$1.006\sin(0.5525t + \Omega_3)$	$.610\sin(0.8925t + \Omega_7)$	$.296\sin(1.2325t + \Omega_{11})$
$1.006\sin(0.6375t + \Omega_4)$	$.503\sin(0.9775t + \Omega_8)$	$.253\sin(1.3175t + \Omega_{12})$

and for the 10 knot case, the 15 sine waves are

$.198\sin(0.4675t + \gamma_1)$	$.753\sin(0.8925t + \gamma_6)$	$.433\sin(1.3175t + \gamma_{11})$
$.497\sin(0.5525t + \gamma_2)$	$.683\sin(0.9775t + \gamma_7)$	$.387\sin(1.3025t + \gamma_{12})$
$.722\sin(0.6375t + \gamma_3)$	$.613\sin(1.0625t + \gamma_8)$	$.351\sin(1.4875t + \gamma_{13})$

$$.811\sin(0.7225t + \gamma_4) \quad .546\sin(1.1475t + \gamma_9) \quad .317\sin(1.5725t + \gamma_{14})$$

$$.805\sin(0.8075t + \gamma_5) \quad .485\sin(1.2325t + \gamma_{10}) \quad .287\sin(1.6515t + \gamma_{15})$$

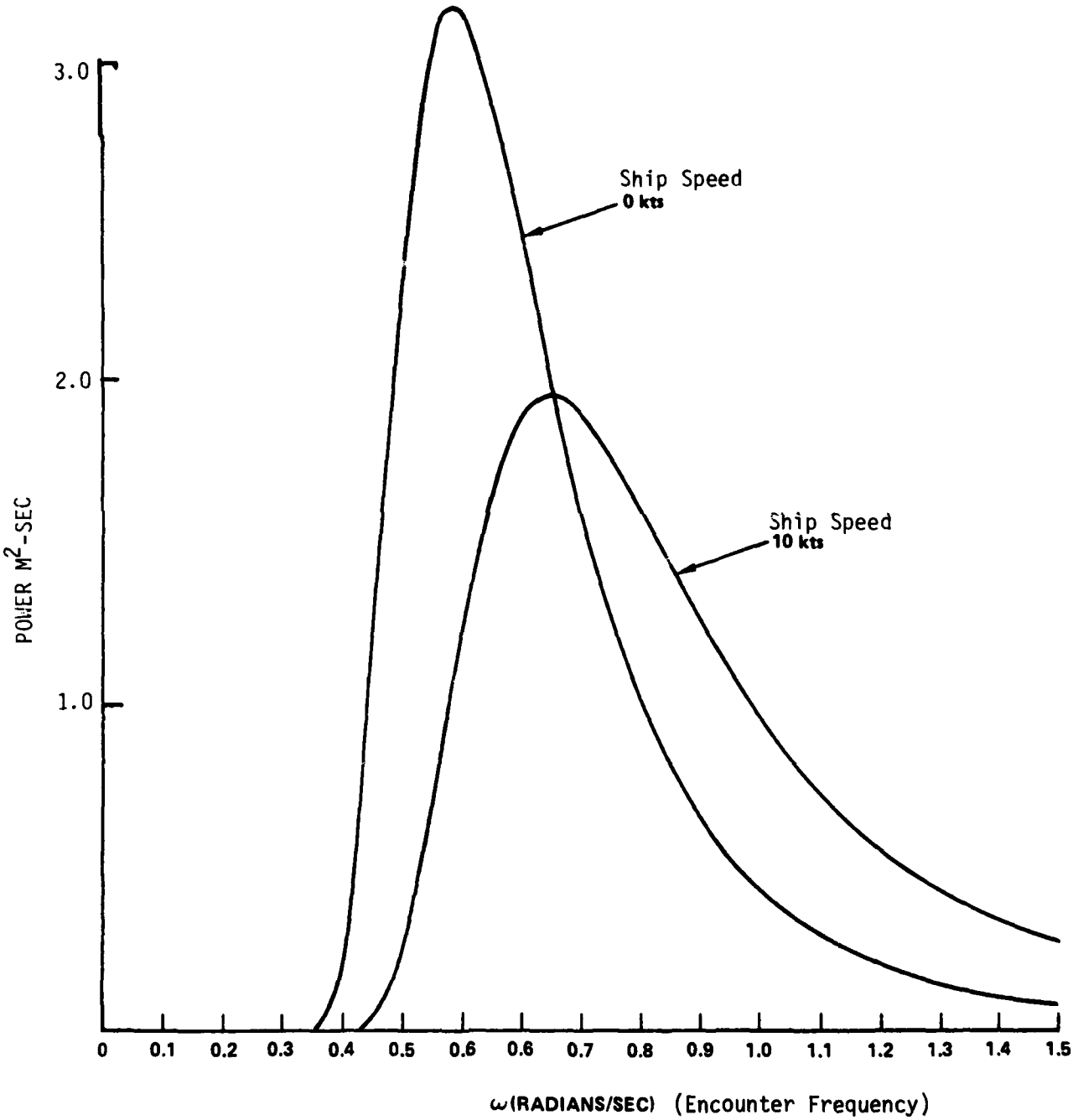

Figure 14 - Pierson-Moskovitz Energy Spectra for a Sea State 6

The forces and moments corresponding to each of the 15 sine waves (per meter wave amplitude) are, for the 10 knots case

FORCES (N)

$1287078\sin(0.4675t+0.0378+\gamma_1)$

$1096017\sin(0.5525t+0.0727+\gamma_2)$

$919726\sin(0.6375t+0.1087+\gamma_3)$

$766055\sin(0.7225t+0.1454+\gamma_4)$

$651706\sin(0.8075t+0.1789+\gamma_5)$

$550677\sin(0.8925t+0.0504+\gamma_6)$

$428417\sin(0.9775t+0.0436+\gamma_7)$

$382384\sin(1.0625t+0.0328+\gamma_8)$

$381785\sin(1.1476t+0.0004+\gamma_9)$

$417333\sin(1.2325t-0.0383+\gamma_{10})$

$478880\sin(1.3175t-0.0725+\gamma_{11})$

$554157\sin(1.4025t-0.0998+\gamma_{12})$

$630444\sin(1.4875t-0.1237+\gamma_{13})$

$698264\sin(1.5725t-0.1554+\gamma_{14})$

$750755\sin(1.6575t-0.2645+\gamma_{15})$

MOMENTS (N-M)

$5132690\sin(0.4675t-1.7093+\gamma_1)$

$4604980\sin(0.5525t-1.7184+\gamma_2)$

$3277861\sin(0.6375t-1.7003+\gamma_3)$

$1460695\sin(1.7225t-1.6242+\gamma_4)$

$885429\sin(0.8075t+1.7104+\gamma_5)$

$4195827\sin(0.8925t+1.5856+\gamma_6)$

$7348714\sin(0.9775t+1.5098+\gamma_7)$

$10133452\sin(1.0625t+1.4806+\gamma_8)$

$12246073\sin(1.1475t+1.4622+\gamma_9)$

$13394644\sin(1.2325t+1.4484+\gamma_{10})$

$13418266\sin(1.3175t+1.4367+\gamma_{11})$

$12064673\sin(1.4025t+1.4260+\gamma_{12})$

$9508579\sin(1.4875t+1.4161+\gamma_{13})$

$5830657\sin(1.5725t+1.4152+\gamma_{14})$

$1408949\sin(1.675t+1.8505+\gamma_{15})$

For the 0 knot case, the forces and moments are

FORCES (N)

$1372533\sin(0.3825t+1.2741+\Omega_1)$

$1089057\sin(0.4675t+0.0508+\Omega_2)$

$843439\sin(0.5525t+0.1015+\Omega_3)$

$647231\sin(0.6375t+0.1485+\Omega_4)$

$540120\sin(0.8925t+0.0113+\Omega_7)$

$586240\sin(0.9775t-0.0394+\Omega_8)$

$601871\sin(1.0625t-0.0698+\Omega_9)$

$497231\sin(1.1475t-0.0827+\Omega_{10})$

FORCE (N)(CONT)

$521593\sin(0.7225t+0.1665+\Omega_5)$ $254421\sin(1.2325t-0.0487+\Omega_{11})$

$495974\sin(0.8075t+0.1553+\Omega_6)$ $62103\sin(1.3175t+2.5599+\Omega_{12})$

MOMENTS (N-M)

$2128444\sin(0.3825t-1.7810+\Omega_1)$ $793793\sin(0.8925t+1.4880+\Omega_7)$

$1310672\sin(0.4675t-1.6365+\Omega_2)$ $469189\sin(0.9775t+1.4271+\Omega_8)$

$662579\sin(0.5525t+0.9815+\Omega_3)$ $1976727\sin(1.0625t-1.5676+\Omega_9)$

$3423026\sin(0.6375t+1.2786+\Omega_4)$ $950234\sin(1.1475t-1.6881+\Omega_{10})$

$6074010\sin(1.7225t+1.3157+\Omega_5)$ $1447324\sin(1.2325t-1.7145+\Omega_{11})$

$7705720\sin(0.8075t+1.4132+\Omega_6)$ $1397494\sin(1.3175t-1.7153+\Omega_{12})$

DTNSRDC ISSUES THREE TYPES OF REPORTS

1. DTNSRDC REPORTS, A FORMAL SERIES, CONTAIN INFORMATION OF PERMANENT TECHNICAL VALUE. THEY CARRY A CONSECUTIVE NUMERICAL IDENTIFICATION REGARDLESS OF THEIR CLASSIFICATION OR THE ORIGINATING DEPARTMENT.

2. DEPARTMENTAL REPORTS, A SEMIFORMAL SERIES, CONTAIN INFORMATION OF A PRELIMINARY, TEMPORARY, OR PROPRIETARY NATURE OR OF LIMITED INTEREST OR SIGNIFICANCE. THEY CARRY A DEPARTMENTAL ALPHANUMERICAL IDENTIFICATION.

3. TECHNICAL MEMORANDA, AN INFORMAL SERIES, CONTAIN TECHNICAL DOCUMENTATION OF LIMITED USE AND INTEREST. THEY ARE PRIMARILY WORKING PAPERS INTENDED FOR INTERNAL USE. THEY CARRY AN IDENTIFYING NUMBER WHICH INDICATES THEIR TYPE AND THE NUMERICAL CODE OF THE ORIGINATING DEPARTMENT. ANY DISTRIBUTION OUTSIDE DTNSRDC MUST BE APPROVED BY THE HEAD OF THE ORIGINATING DEPARTMENT ON A CASE-BY-CASE BASIS.